Figure S1

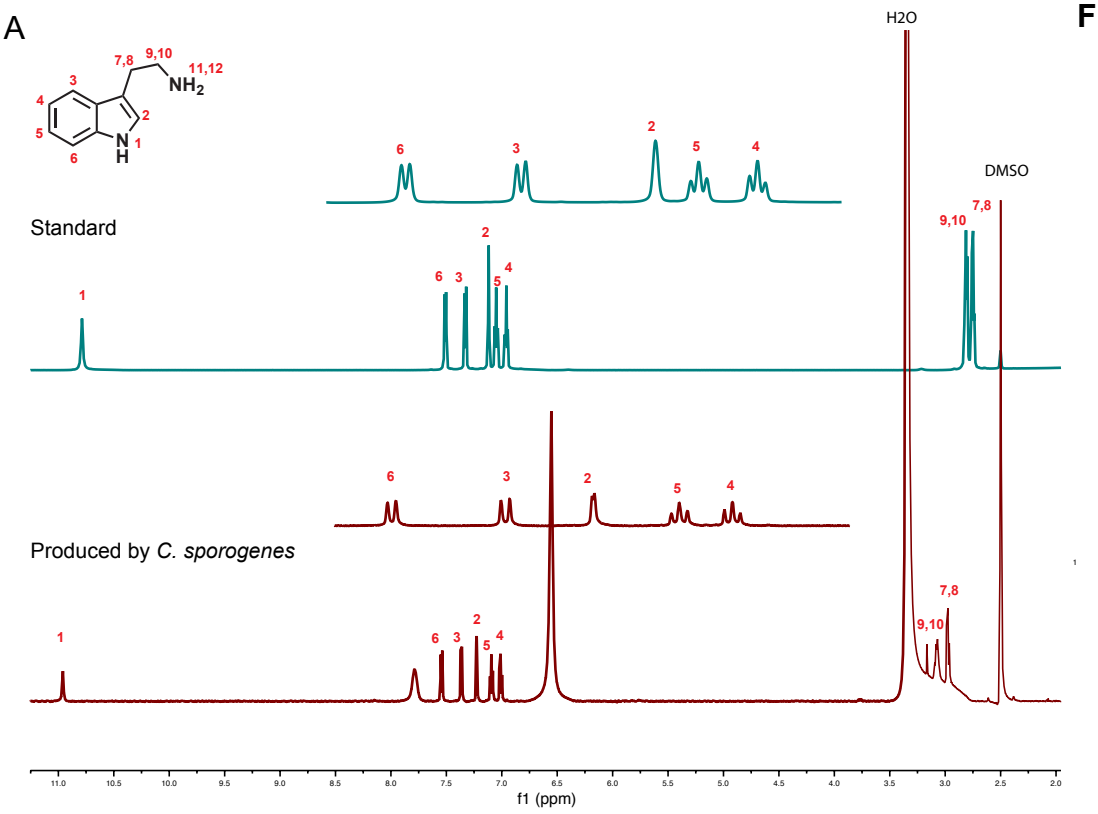
A
H2O
DMSO
Standard
Produced by C. sporogenes
f1 (ppm)

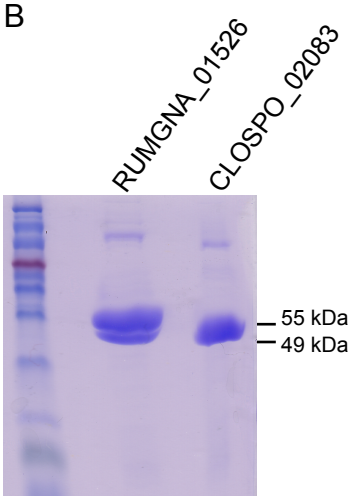
B
RUMGNA_01526
CLOSPO_02083
55 kDa
49 kDa

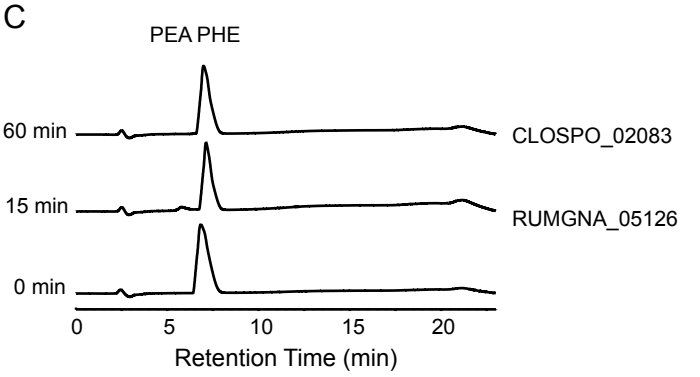
C
PEA PHE
60 min
15 min
0 min
CLOSPO_02083
RUMGNA_05126
Retention Time (min)

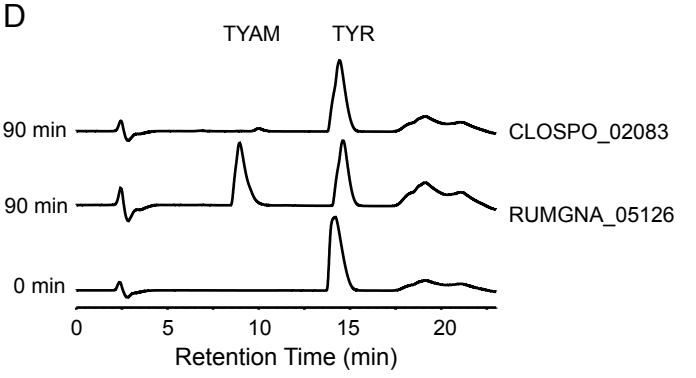
D
TYAM
TYR
90 min
90 min
0 min
CLOSPO_02083
RUMGNA_05126
Retention Time (min)

Figure S2

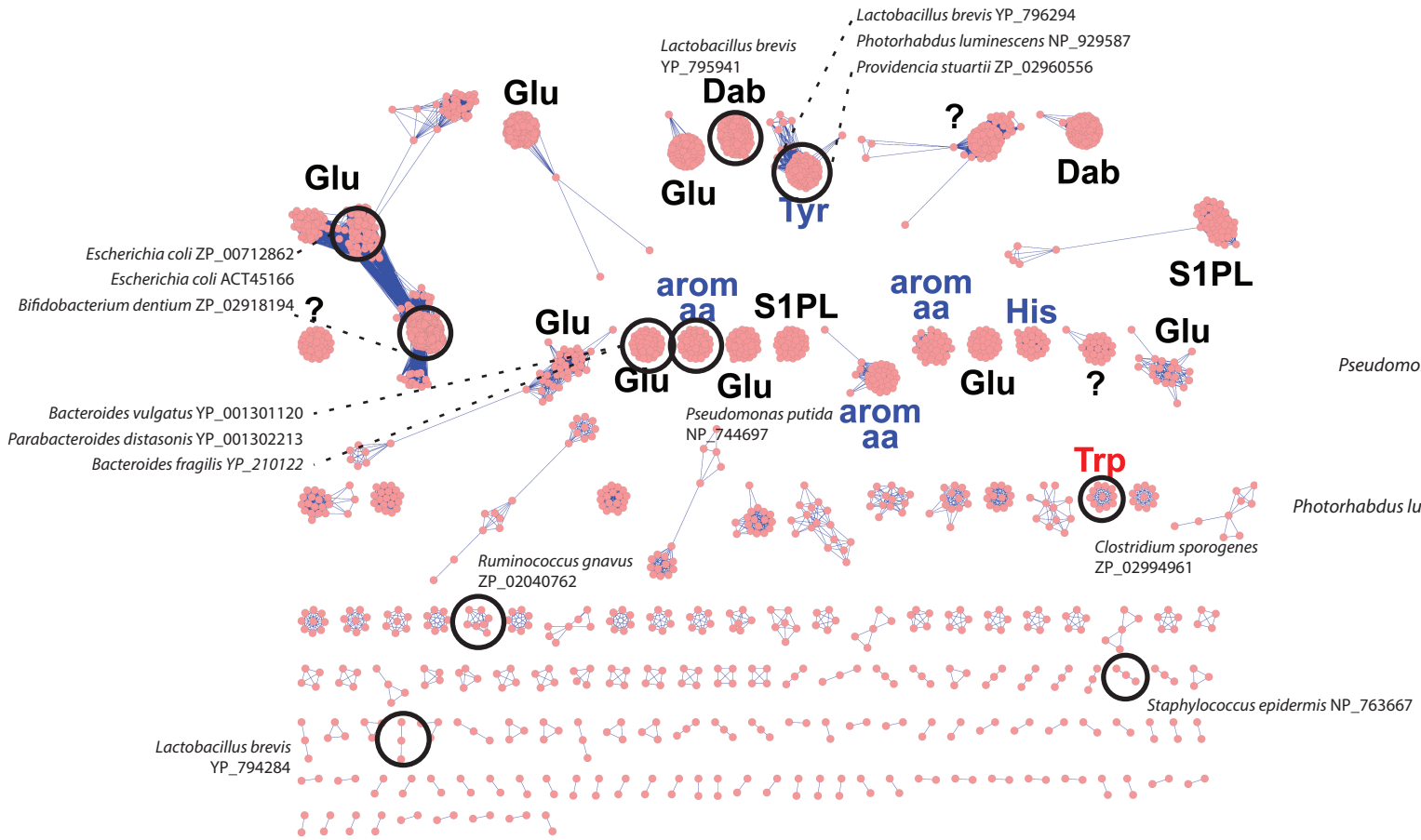
Lactobacillus brevis YP_796294
Photorhabdus luminescens NP_929587
Providencia stuartii ZP_02960556
Lactobacillus brevis YP_795941
Dab
Glu
Tyr
?
Dab
Glu
S1PL
arom aa
arom aa
His
Glu
Escherichia coli ZP_00712862
Escherichia coli ACT45166
Bifidobacterium dentium ZP_02918194
?
Glu
Glu
Glu
Glu
?
Bacteroides vulgatus YP_001301120
Parabacteroides distasonis YP_001302213
Bacteroides fragilis YP_210122
Pseudomonas putida NP_744697
arom aa
Trp
Clostridium sporogenes ZP_02994961
Ruminococcus gnavus ZP_02040762
Staphylococcus epidermis NP_763667
Lactobacillus brevis YP_794284

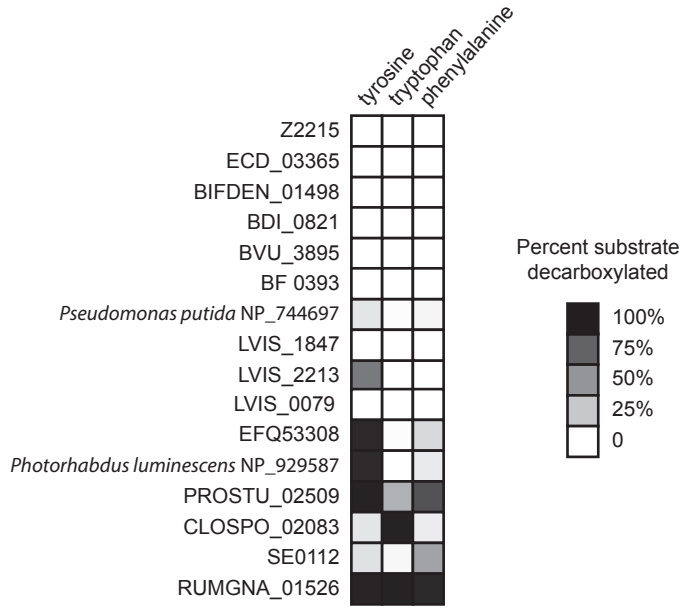
tyrosine
tryptophan
phenylalanine
Z2215
ECD_03365
BIFDEN_01498
BDI_0821
BVU_3895
BF 0393
Pseudomonas putida NP_744697
LVIS_1847
LVIS_2213
LVIS_0079
EFQ53308
Photorhabdus luminescens NP_929587
PROSTU_02509
CLOSPO_02083
SE0112
RUMGNA_01526
Percent substrate decarboxylated
100%
75%
50%
25%
0

Figure S3

A

	CLOSPO_02083 Tryptophan	RUMGNA_01526 Tryptophan	RUMGNA_01526 Phenylalanine
K_m (mM)	2.8 ± 0.03	1.1 ± 0.07	70 ± 6.6
v_{max} (mM/min)	0.12 ± 0.00	0.04 ± 0.00	0.12 ± 0.01
k_{cat} (min^{-1})	1200	4400	230
k_{cat}/K_m ($M^{-1}sec^{-1}$)	7.3 x 10^3	6.8 x 10^4	56

B

	CLOSPO_02083 Tryptophan	RUMGNA_01526 Tryptophan	RUMGNA_01526 Phenylalanine
$K_{0.5}$ (mM)	2.13 ± 0.03	0.76 ± 0.03	23 ± 1.2
v_{max} (mM/min)	0.11 ± 0.00	0.04 ± 0.00	0.06 ± 0.00
h	1.5	1.7	2.7

C

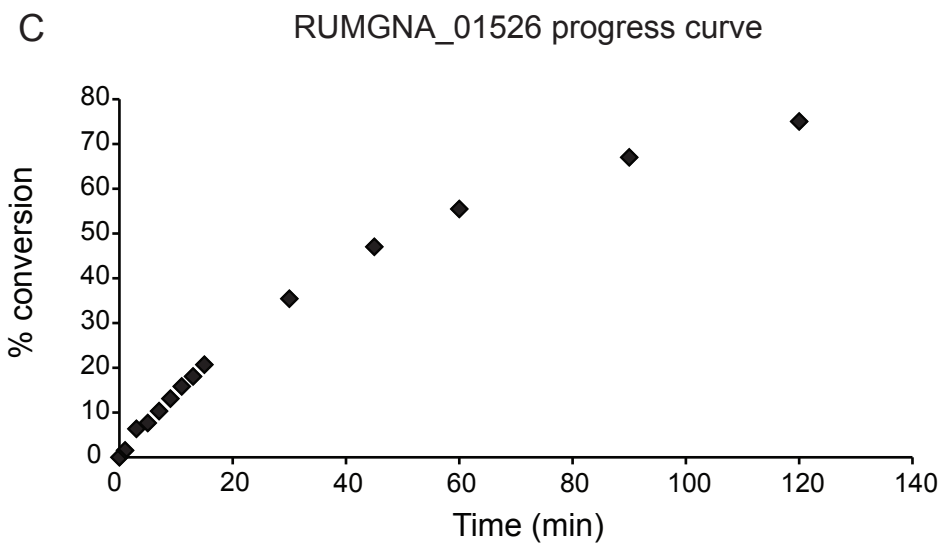

Figure S4

A

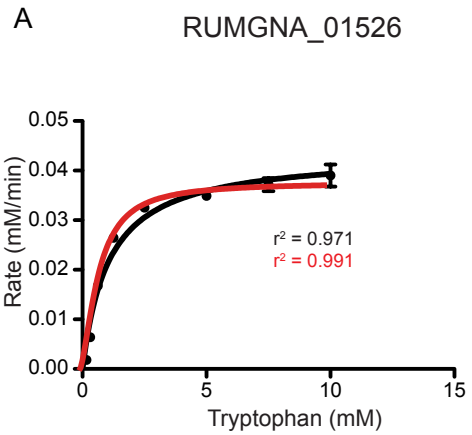

B

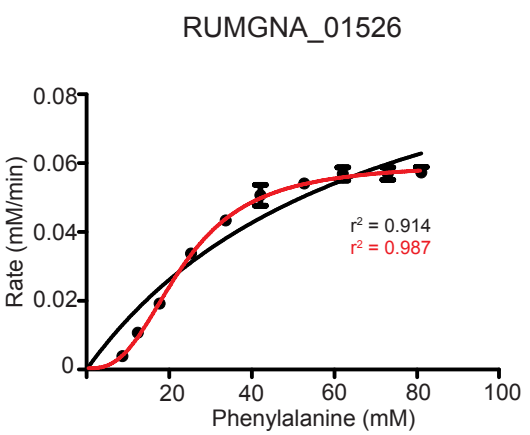

C

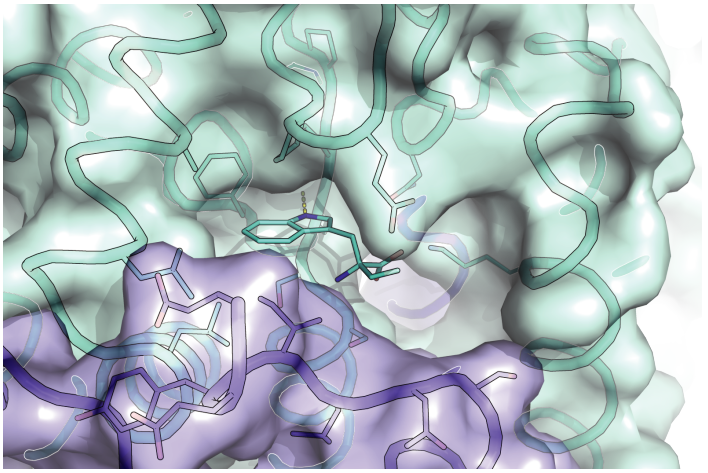

Figure S5

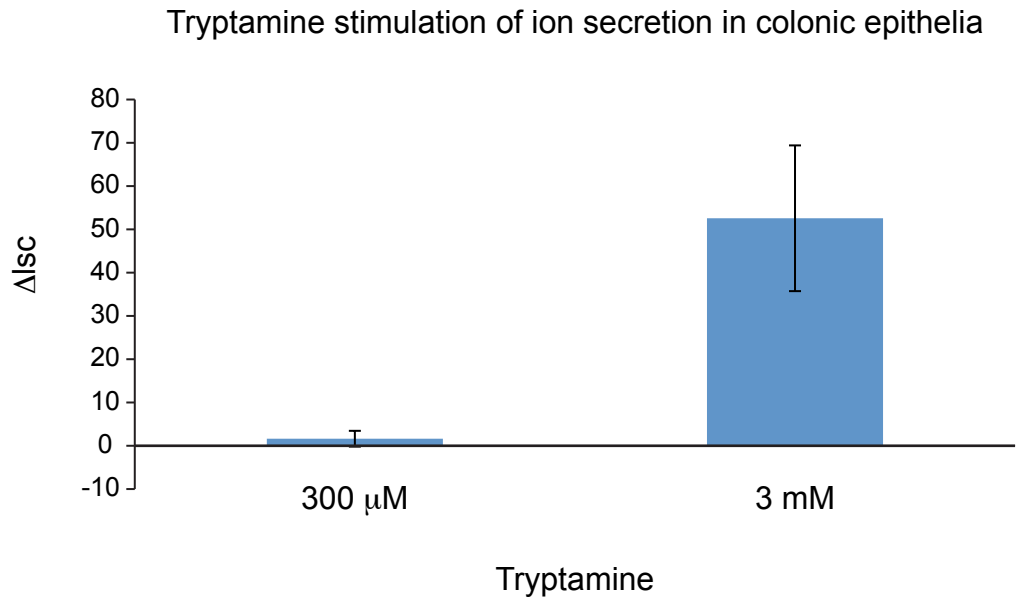
Tryptamine stimulation of ion secretion in colonic epithelia
80
70
60
50
40
30
20
10
0
-10
ΔIsc
300 μM
3 mM
Tryptamine

Figure S6

A

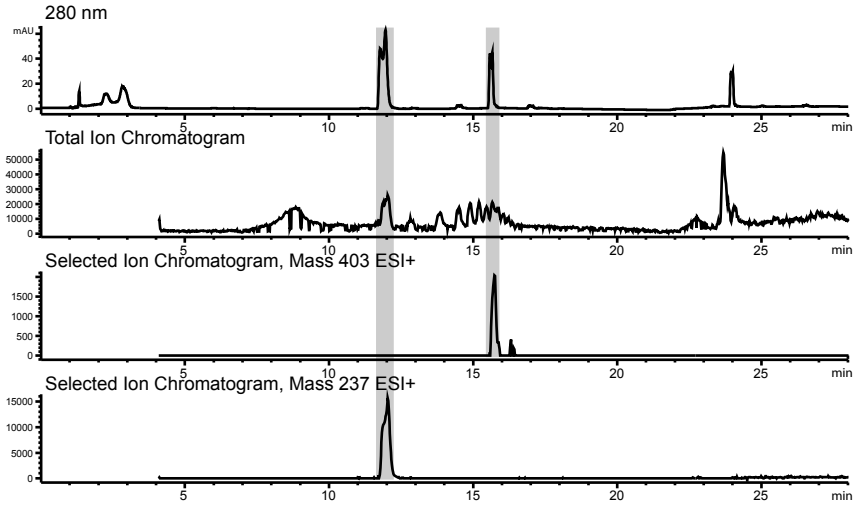

B

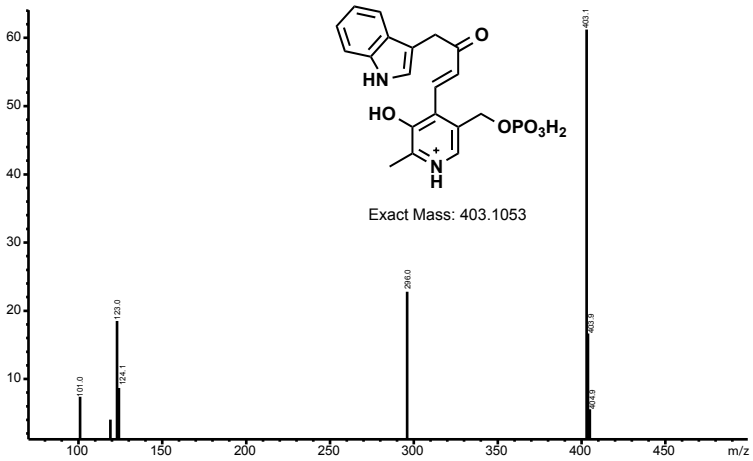

C

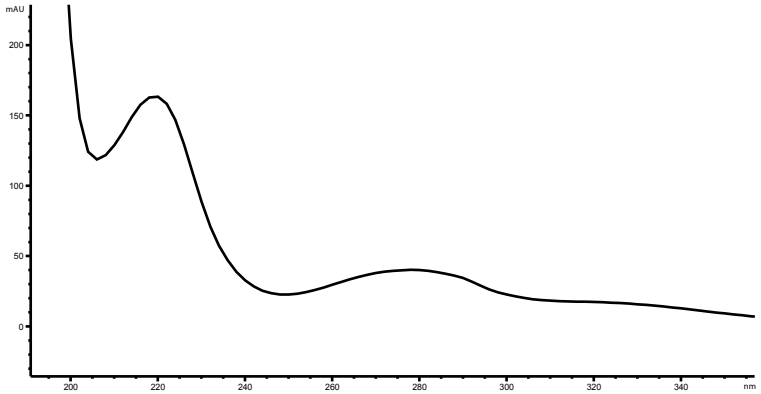

D

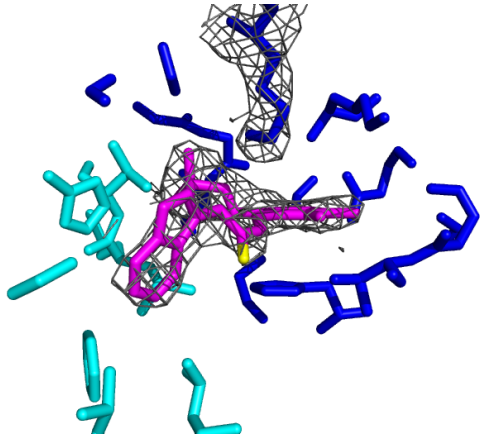

Supplemental Figure Legends

Figure S1 related to Figure 1. Characterization of tryptamine production. (A) NMR of *C. sporogenes* produced tryptamine compared to standard (Sigma-Aldrich). Standard tryptamine is shown in teal, and *C. sporogenes*-produced tryptamine is shown in burgundy. (B) SDS-PAGE of purified CLOSPO_02083 and RUMGNA_01526. Using a BioRad ReadyGel, Precast SDS-PAGE 10% Tris-HCl, 1 μL of purified protein was loaded. Lane 1: Precision Plus Protein Prestained Standards, Dual Color, Lane 2: RUGMNA_01526 55 kDa, Lane 3: CLOSPO_02083 49 kDa. (C, D) Biochemical activity of CLOSPO_02083 and RUMGNA_01526 with phenylalanine and tyrosine substrates. HPLC traces for (C) phenylalanine or (D) tyrosine decarboxylation by CLOSPO_02083 or RUMGNA_01526.

Figure S2 related to Figure 2. Cytoscape clustering of pfam00282 containing sequences in the JGI database and activity of selected enzymes. (A) The pfam consensus sequence for PLP-dependent decarboxylases (PLP_dec, pfam00282) was used as a query in a BLAST search against the JGI database and hits were clustered based on similarity. Clusters are labeled with predicted substrates. Genes included in this study were selected to represent several clusters and are labeled. (B) Summary of decarboxylase activity. Genes were cloned into pET-28a and expressed in *E. coli* BL21 in the presence of tryptophan, tyrosine, or phenylalanine for 24 hours. Percent decarboxylation was determined by dividing the integrated peak area (AUC) of the amine by the sum of the AUC of both the amine and acid, and represented in gray scale.

Figure S3 related to Figure 4. Table of kinetic results. (A) Michaelis-Menten and (B) Hill equation kinetic parameters for CLOPSO_02083 and RUMGNA_01526 with tryptophan and

RUMGNA_01526 with phenylalanine. (C) Progress curve of tryptophan consumption by 10 nM RUMGNA_01526 in the presence of 1.25 mM tryptophan.

Figure S4 related to Figure 3. Hill equation fit to RUMGNA_01526 kinetic data. Rate (mM tryptamine/min) vs substrate concentration curves for (A) tryptophan or (B) phenylalanine decarboxylation by RUMGNA_01526 100 nM enzyme incubated with tryptophan varied from 0.15-24.5 mM. GraphPad was used to fit the Michaelis-Menten (black) and Hill (red) equations. (C) Allosteric site shows free (*S*)-α-FMT buried in a hydrophobic pocket near the N-terminus of the enzyme.

Figure S5 related to Figure 1. Tryptamine stimulates ion secretion by intestinal epithelial cells. Segments of proximal-mid colon, stripped of external muscle layers, were exposed to either 300 μM or 3 mM tryptamine using the Ussing chamber. The change in short circuit current was determined. A significant increase in ion secretions was observed in the presence of 3 mM but not 300 μM tryptamine.

Figure S6 related to Figure 3. Structure determination of (*S*)-α-FMT-PLP adduct (A) 280 nm UV trace, total ion chromatogram, and selected ion chromatograms for the released adduct. (B) Mass spectrum of adduct shows a compound with a mass of 403, corresponding to the structure shown in the inset. (C) UV-Vis spectrum of adduct. (D) Electron density shows clear separation of adduct and lysine residue.

Table S1 Data collection and refinement statistics

	Apo-RUMGNA_01526	S-aFMT-RUMGNA_01526
Wavelength (Å)		
Resolution range (Å)	79.37 - 2.804 (2.905 - 2.804)	52.44 - 2.84 (2.942 - 2.84)
Space group	P 1	P 41 21 2
Unit cell	58.63 145.77 165.07 72.85 88.84 88.3	135.03 135.03 249.8 90 90 90
Total reflections	218936 (22174)	730528 (73919)
Unique reflections	121102 (12262)	55248 (5448)
Multiplicity	1.8 (1.8)	13.2 (13.6)
Completeness (%)	94.70 (96.28)	99.97 (99.96)
Mean I/sigma(I)	9.54 (2.09)	25.80 (3.80)
Wilson B-factor	41.16	54.76
R-merge	0.08033 (0.363)	0.119 (0.8652)
R-meas	0.1136	0.1238
CC1/2	0.99 (0.73)	0.999 (0.881)
CC*	0.998 (0.919)	1 (0.968)
R-work	0.2311 (0.3077)	0.2098 (0.2745)
R-free	0.2568 (0.3623)	0.2423 (0.3494)
Number of atoms	29598	15146
macromolecules	29064	14886
ligands	120	184
water	414	0
Protein residues	3696	1889
RMS(bonds)	0.002	0.007
RMS(angles)	0.67	0.64
Ramachandran favored (%)	96	95
Ramachandran outliers (%)	0	0.053
Clashscore	3.03	3.04
Average B-factor	21.2	36.4
macromolecules	21.3	36.2
ligands	41.8	47.9
solvent	9.7	

Statistics for the highest-resolution shell are shown in parentheses.

Experimental Procedures

Cloning candidate decarboxylase genes. Candidate decarboxylase genes were cloned from genomic DNA prepared from each strain using Phusion High Fidelity DNA Polymerase (NEB). PCR products were purified (MinElute, Qiagen) and used directly as primers in a CPEC reaction with pET-28a (Novagen) that had previously been digested with *Nde*I and *Xho*I (98°C for 30 s; 6 cycles of 98°C for 10 s, 55°C for 30 s, 72°C for 3 min; 72°C for 5 min). The identities of the resulting pET-28a-*decarboxylase* constructs were confirmed by DNA sequencing.

HPLC analysis of culture fluid from *E. coli* expressing putative decarboxylases. Samples of cell-free supernatant containing tryptophan, phenylalanine, or tyrosine were analyzed on an Agilent 1200 series HPLC equipped with a diode array detector using a ThermoScientific Hypercarb column (100 mm x 4.6 mm x 5 μm) at a flow rate of 1.0 ml/min at ambient temperature. There were four mobile phase solvents: (A) water, (B) acetonitrile, (C) isopropanol, and (D) methanol, each supplemented with 0.1% TFA (trifluoroacetic acid). The elution gradient had the following profile: 5.0-30.8% B, 5.0-30.8% C, and 2.0% D from 0-14 min; 30.8-49.0% B, 30.8-49.0% C, 2.0% D from 14-17 min; and 49.0-5.0% B, 49.0-5.0% C, 2.0% D from 17-20 min;

5.0% B, 5.0% C, 2.0% D from 20-23 min. Standard elution times were as follows: tryptophan 13.0 min (monitored at 280 nm), tryptamine 11.0 min (280 nm); phenylalanine 6.9 min (220 nm), phenethylamine 5.6 min (220 nm), tyrosine 6.8 min (220 nm), tyramine 5.1 min (220 nm).

Kinetic characterization of CLOSPO_02083 and RUMGNA_01526 activity with aromatic amino acid substrates. Reaction mixtures contained 50 mM sodium phosphate pH 6.5, 300 mM NaCl, and 40 μM PLP. Reactions were initiated by the addition of enzyme and terminated by quenching aliquots with 1 volume of MeOH and performed at 37°C. All substrates purchased from Sigma-Aldrich.

To determine the kinetic parameters for the decarboxylation of tryptophan by RUMGNA_01526, RUMGNA_01526 was added to a final concentration of 10 nM, and k_{cat} and K_m were determined by varying the concentration of tryptophan from 0.15-10 mM. Reactions proceeded for 7 min and were quenched as described. 100 μl of the quenched reaction was analyzed by HPLC. Peak areas were integrated and compared with a standard curve to calculate product concentration. Triplicate measurements were made from a single batch of purified enzyme. Initial velocity data were fit to the Michaelis-Menten equation by using the program GraphPad. The allosteric sigmoidal model was used by fitting to the Hill equation: $y=v_{max}*x^h/(K_{0.5}{}^h+x^h)$, where h is the Hill coefficient and $K_{0.5}$ is the apparent concentration at half maximal velocity.

Under the same buffer and reaction conditions, the kinetic parameters for the decarboxylation of phenylalanine by RUMGNA_01526 were determined by adding RUMGNA_01526 to a final concentration of 500 nM and the concentration of phenylalanine varied from 5-80 mM. Reactions proceeded for 10 min. The kinetic parameters for the decarboxylation of tryptophan by CLOSPO_02083 were determined by adding CLOSPO_02083 to a final concentration of 100 nM and the concentration of tryptophan varied from 0.15-24.5

mM; reactions proceeded for 6 minutes. Decarboxylation of phenylalanine by CLOSPO_02083 was not observed under saturation conditions using 1 μM enzyme and 90mM substrate for 60 minutes. Decarboxylation of tyrosine by RUMGNA_01526 and CLOSPO_02083 was observed using 1 μM enzyme with 2.28 mM tyrosine for 90 minutes.

Experiments with the inhibitor (*S*)-α-FMT were performed by analyzing product formation over time after the addition of (*S*)-α-FMT to pre-incubated enzyme and substrate at a concentration of 3*K_m (2.5 mM Trp for RUMGNA_01526, and 10 mM Trp for CLOSPO_02083). Progress curves were fitted to the equation $[P]=(v_i/k_{obs})(1-\exp(-k_{obs}t))$, where *P* is the product formed at time *t*, v_i is the initial velocity, and k_{obs} is the apparent first-order rate constant for enzyme inactivation. The k_{obs} were plotted versus inhibitor concentration and fitted to the equation $k_{obs}=k_{inact}[I]/(K_{app}+[I])$, where K_{app} is the apparent dissociation constant of the reversible enzyme-inhibitor complex, and k_{inact} is the first-order rate constant for apparent irreversible conversion of the enzyme-inhibitor complex to covalently bound complex. K_i values were calculated using the equation $K_i=K_{app}/(1+[\text{tryptophan}])/K_{m,Trp}$) using experimentally determined K_m values for tryptophan (32).

Ion secretion from the murine colon. A segment of proximal-mid colon, stripped of external muscle layers from each of three SvEv129 mice was mounted in 0.3 cm^2 area, 4 mL Ussing chamber. Change in short circuit current (Δ Isc) was determined in response to two concentrations of tryptamine (300 μM and 3mM) on the mucosal side to mimic bacterially produced tryptamine.

Phylogenetic analysis of microbial decarboxylases. Multiple sequence alignments were generated using MAFFT server (33), using Mafft-homologs function and the Blosum62 scoring matrix. Additionally, we used a structure-based sequence alignment of four decarboxylases (the holo structure of RUMGNA_01526 presented here and the following three structures from the:

3F9T, 3FZ8, and 4E1O) as a constraint in the alignment procedure. The structure-based sequence alignment was generated by "Match->Align" function in Chimera (34), followed by manual refinement. The phylogenetic tree was generated using the PHYLIP Neighbor Joining method (http://evolution.genetics.washington.edu/phylip.html), with the Jones-Taylor-Thornton distance matrix model.

Metagenomic analysis of decarboxylase prevalence. Protein databases of all assembled metagenomic data of the Human Microbiome Project stool samples were accessed through HMP Data Analysis and Coordination Center. BLASTP searches were performed using RUMGNA_01526 and CLOSPO_02083 as query sequences**,** with a cutoff expectation value of $1e^{-50}$ in protein sequences bigger than 100 amino acids. Hits were then analyzed further by comparing them to the NCBI protein database using BLASTP and determining their closest homologs in sequenced microbial genomes.

Supplemental References

32. Schirmer A, Kennedy J, Murli S, Reid R, & Santi DV (2006) Targeted covalent inactivation of protein kinases by resorcylic acid lactone polyketides. *Proc Natl Acad Sci USA* 103(11): 4234-4239.
33. Katoh K & Standley DM (2014) MAFFT: iterative refinement and additional methods. *Methods in molecular biology* 1079:131-146.
34. Pettersen EF*, et al.* (2004) UCSF Chimera--a visualization system for exploratory research and analysis. *Journal of computational chemistry* 25(13):1605-1612.